

SUB-THZ RADIATION MECHANISMS IN SOLAR FLARES

GREGORY D. FLEISHMAN^{1,2} AND EDUARD P. KONTAR³

Draft version February 5, 2020

ABSTRACT

Observations in the sub-THz range of large solar flares have revealed a mysterious spectral component increasing with frequency and hence distinct from the microwave component commonly accepted to be produced by gyrosynchrotron (GS) emission from accelerated electrons. Evidently, having a distinct sub-THz component requires either a distinct emission mechanism (compared to the GS one), or different properties of electrons and location, or both. We find, however, that the list of possible emission mechanisms is incomplete. This Letter proposes a more complete list of emission mechanisms, capable of producing a sub-THz component, both well-known and new in this context and calculates a representative set of their spectra produced by a) free-free emission, b) gyrosynchrotron emission, c) synchrotron emission from relativistic positrons/electrons, d) diffusive radiation, and e) Cherenkov emission. We discuss the possible role of the mechanisms in forming the sub-THz emission and emphasize their diagnostics potential for flares.

Subject headings: Sun: flares—acceleration of particles—turbulence—diffusion—Sun: magnetic fields—Sun: radio radiation

1. INTRODUCTION

Solar flares, being manifestations of prompt energy releases, produce electromagnetic radiation throughout the entire spectrum of electromagnetic emission from radio waves to gamma rays (e.g. Dennis & Schwartz 1989; Brown & Kontar 2005). Although the radio, UV, X-ray, and gamma-ray emission is generally well observed with high resolution from huge number of events, the sub-THz radiation has only recently been observed from a few large events, at a small number of frequencies (Kaufmann et al. 2001; Trotter et al. 2002; Lüthi et al. 2004a,b; Kaufmann et al. 2004; Cristiani et al. 2008; Trotter et al. 2008; Kaufmann et al. 2009b,a; Silva et al. 2007). The available observational tools are unable to measure polarization and are clearly insufficient to provide detailed spectral and positional information about the sub-THz bursts. Nevertheless, available sub-THz observations have already provided us with puzzling questions which have yet to be answered.

The observations suggest that, on top of quiet Sun emission, at least two kinds of sub-THz emission can be produced. The first kind looks like a natural extension of the microwave spectrum at higher frequencies and so can reasonably be interpreted as synchrotron radiation from accelerated electrons, which are also responsible for microwave and hard X-ray emission. The second kind looks like a distinct spectral component rising with frequency in the sub-THz range in contrast to the microwave spectrum, which falls with frequency. The origin of this component is un-

clear; there is no consensus about the possible emission mechanism producing it, moreover, it is ambiguous whether the emission is of thermal or nonthermal origin.

The main observational characteristics of this component are: relatively large radiation peak flux of the order of 10^4 sfu (Kaufmann et al. 2004); radiation spectrum rising with frequency $F(f) \propto f^\delta$; spectral index varying with time within $\delta \sim 1 \dots 6$; sub-THz component can display a sub-second time variability with the modulation about 5% (Kaufmann et al. 2009a); the source size is believed to be less than $20''$, however, this conclusion is based on a multi-beam observation of a few antennas with $\sim 4'$ resolution each, rather than on true imaging; therefore, the size estimate must be considered with caution. In addition, observations (Lüthi et al. 2004a,b) suggest the existence of both compact $\sim 10''$ and extended $\sim 60''$ components, and source sizes increasing with frequency.

The emission mechanisms proposed so far to account for the sub-THz component are thermal free-free emission, GS emission from flare accelerated electrons, and synchrotron emission from nuclear decay-generated relativistic positrons (e.g. Nindos et al. 2008, as a review). None of these mechanisms is readily consistent with the full list of the sub-THz component properties and/or with available context observations at other wavelength. Below we analyze these options and also consider two other emission mechanisms capable of producing a spectrum rising with frequency—diffusive radiation in Langmuir (DRL) waves (e.g. Fleishman & Toptygin 2007a,b) and Vavilov-Cherenkov emission (e.g., Bazylev & Zhevago 1987) from chromospheric layers, which make the list of options more complete. Calculating the spectrum from all of the above mentioned models, we establish the range of main source param-

¹ Center for Solar-Terrestrial Research, New Jersey Institute of Technology, Newark, NJ 07102; gfeishm@njit.edu

² Ioffe Physical-Technical Institute of the Russian Academy of Sciences, St. Petersburg 194021, Russia

³ Department of Physics and Astronomy, University of Glasgow, G12 8QQ, United Kingdom

eters for each model emphasizing the strengths and weaknesses of each emission mechanism.

2. FREE-FREE EMISSION

Perhaps the simplest example of a radio spectrum rising with frequency is optically thick thermal free-free emission. Having a rising spectrum from a compact ($\lesssim 20''$) source requires obviously that the source is relatively dense ($n_e \gtrsim 10^{11} \text{ cm}^{-3}$) and hot ($T_e \gtrsim 10 \text{ MK}$). From available X-ray observations (e.g. Dennis & Schwartz 1989; Kašparová et al. 2005), we can exclude the option of a source that is simultaneously dense and hot, say $n_e \sim 10^{12} \text{ cm}^{-3}$ and $T_e \sim 10 \text{ MK}$, $EM = n_e^2 V \sim 3 \times 10^{51} \text{ cm}^{-3}$, since a plasma with the corresponding emission measure and temperature would produce stronger X-ray emission than is actually observed from solar flares (Dennis & Schwartz 1989; Emslie et al. 2003; Brown et al. 2007). We cannot exclude, however, dense plasmas of lower temperature, $T_e \sim 1 \text{ MK}$; such plasmas do not contradict to the current X-ray and UV observations.

Figure 1 shows free-free spectra from overdense sources with temperature around 1 MK. Evidently, having a flux density above 1000 sfu level requires thermal electron number density above 10^{12} cm^{-3} or/and the linear size of the source above $20''$. Although available size estimates do not favor sources larger than $20''$, a firm conclusion about that must await true imaging observations at the sub-THz range. Such large emission sources, tens of arcseconds, are consistent with at least some observations (Lüthi et al. 2004a,b).

It should be noted that the spectral index of a spatially uniform source of free-free radiation cannot be larger than 2, while the observations suggest larger values, especially during the initial phase of the sub-THz bursts (Kaufmann et al. 2009b). These larger values can be reconciled with the free-free mechanism if we allow for a cooler dense absorbing layer in the line of sight between the source and observer, providing an attenuation factor $\exp(-\tau_{ff})$, where $\tau_{ff} \propto nn_e(1 - \exp(-hf/kT))T^{-1/2}f^{-3} \propto nn_eT^{-3/2}f^{-2}$ is the free-free optical depth; such a non-uniform source is capable of producing frequency spectra with a very sharp low frequency edge compatible with observations.

Finally, we emphasize that the free-free emission mechanism can display temporal variability. For sausage mode loop oscillations, for example, $B = B_0(1 + m \cos(2\pi t/P))$, with a period P and modulation amplitude $m < 1$, we can calculate all relevant parameter variations and, thus, make firm prediction about the free-free emission modulation amplitude in the optically thick and thin regimes: $F_{thick} \propto (1 + \frac{m}{6} \cos(2\pi t/P))$ and $F_{thin} \propto (1 + \frac{2m}{3} \cos(2\pi t/P))$. Therefore, the optically thick and thin part of the free-free emission oscillate in phase. However, the modulation amplitude in the thin regime is four times larger than in the thick regime.

We can conclude that the free-free model can provide sufficient flux and spectral index consistent with observations of the sub-THz component, although the

source density must be somewhat high compared with standard coronal loop densities.

3. GYROSYNCHROTRON EMISSION FROM A COMPACT SOURCE

Flare generated electrons gyrating in a magnetic field produce strong gyrosynchrotron emission across a broad range of frequencies (e.g. Bastian et al. 1998; Nindos et al. 2008). Silva et al. (2007) have demonstrated that a rising optically thick GS spectrum in the sub-THz range requires a large magnetic field in the emission source; typically, this implies also a large plasma density. Therefore, we include the free-free absorption and emission along with the GS contribution in our calculations. We have investigated the corresponding parameter space and confidently confirm the conclusion of Silva et al. (2007) that only a very compact source $\sim 1''$ with a very strong magnetic field $B > 2000 \text{ G}$, in which all flare accelerated electrons ($N_e[> 50 \text{ keV}] = 5 \cdot 10^{35}$, $n_e[> 50 \text{ keV}] \sim 10^{12} \text{ cm}^{-3}$) simultaneously reside, could be consistent with the spectrum of sub-THz flare component, Figure 2. The number of required electrons is typical for a large (GOES X-class) solar flare (e.g. Brown et al. 2007).

Although this model is consistent with a small source size, it requires more than extreme source parameters. In addition, this model cannot account for large spectral indices (> 3) of the sub-THz component. The Razin effect in a dense plasma with a magnetic field around 800 G was proposed to form a steeper spectrum in the sub-THz range (Silva et al. 2007). However, as seen from Figure 2, the flux density for $B = 800 \text{ G}$ is much lower than observed (in fact, the free-free absorption additionally reduces the flux here). A larger magnetic field (to increase the flux level) will require a proportionally larger thermal electron density to keep the Razin effect in place, which will further increase free-free absorption in the source, so the observed flux level will not be met under conditions of strong Razin effect, Figure 2(b). An increase of the source size above $2''$ with the same total number of fast electrons, magnetic field and thermal electron density results in a spectrum totally dominated by the free-free contribution—the model considered in the previous section.

We note that GS emission model can easily account for the observed temporal pulsations of the sub-THz component via, e.g., loop oscillations at large time scales and/or fluctuations of fast electron injection (Kiplinger et al. 1984; Aschwanden et al. 1998) at various time scales. In addition, good temporal correlation with high energy hard X-rays and gamma-ray continuum will be rather natural. Nevertheless, we feel that unrealistically extreme GS source parameters are needed to reconcile the model with observations of sub-THz emission from large flares. In contrast, weaker sub-THz fluxes $F_f \sim 100 \text{ sfu}$ observed from M-class flares (Cristiani et al. 2008) may agree with the GS emission mechanism.

4. SYNCHROTRON EMISSION FROM RELATIVISTIC POSITRONS

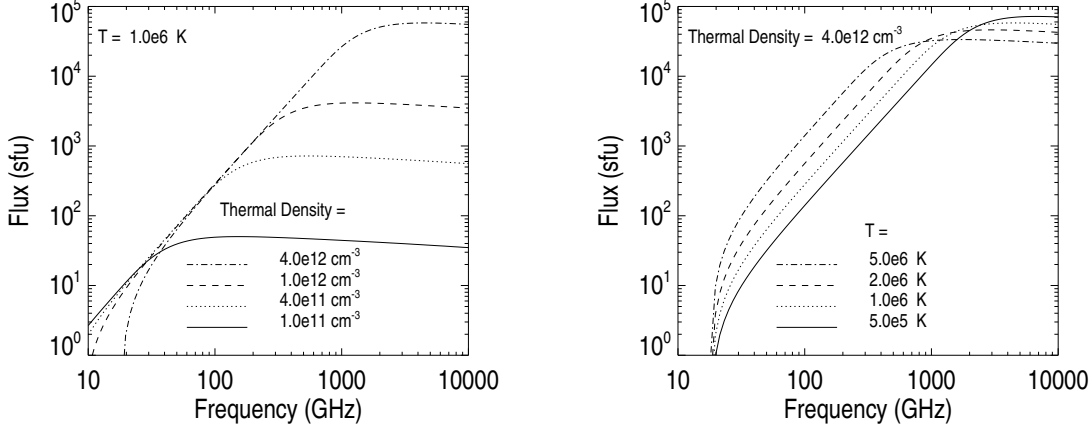


FIG. 1.— Radio spectra produced by thermal free-free emission from a uniform cubic source with a linear size of $20''$ for $n_e = 10^{11} \dots 4 \cdot 10^{12} \text{ cm}^{-3}$ and $T_e = 0.5 \dots 5 \text{ MK}$.

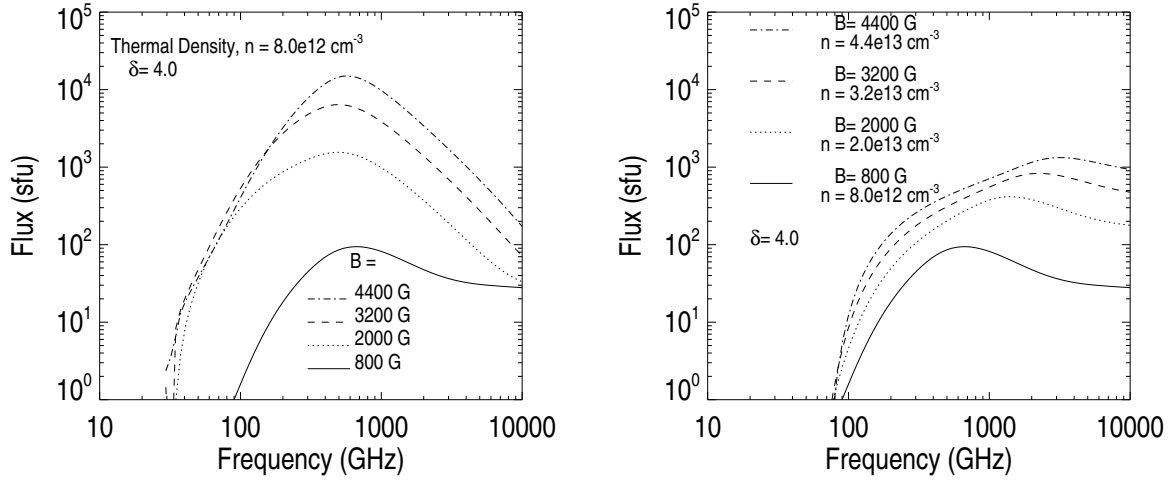


FIG. 2.— (a) Radio spectra produced by GS plus free-free contributions from a uniform source with a size of $1''$ for $n_e = 8 \cdot 10^{12} \text{ cm}^{-3}$ and $B = 800 \dots 4400 \text{ G}$. (b) Razin-suppressed GS spectra with the Razin frequency 200 GHz plus the free-free component.

Flare-accelerated ions of tens MeV or above colliding with thermal ions in dense layers of the solar atmosphere trigger nuclear reactions, with relativistic positrons being one of the products of such interactions (Lingenfelter & Ramaty 1967; Kozlovsky et al. 2002). These relativistic positrons are capable of producing sub-THz synchrotron radiation with a peak frequency around $f_{peak} \sim f_{Be} \gamma^2$, where f_{Be} is the electron gyrofrequency and γ is the Lorenz-factor, as suggested by Lingenfelter & Ramaty (1967).

Although the synchrotron peak frequency can easily fall into the sub-THz or THz range (Trottet et al. 2008) considering typical magnetic field ($B \sim 1000 \text{ G}$) and Lorenz-factors $\gamma \sim 20$, the low-frequency synchrotron spectrum, $F_f \propto f^{1/3}$, Figure 3(a), is inconsistent with the whole range of the observed spectral index values unless we adopt an additional absorption mechanism leading to a sharper spectral shape. The only viable absorption mechanism is free-free absorption, which again requires high plasma density, $\sim 10^{12} \text{ cm}^{-3}$, Figure 3(b). Even though a combination of the synchrotron radiation from relativistic positrons and free-free absorption is capa-

ble of producing the required spectral shape, the correct flux density requires more relativistic positrons than seems to be available from nuclear interactions even in large flares. The total number of energetic protons above 30 MeV for large solar flares as deduced from RHESSI observations is in the range $10^{29} - 10^{33}$ (e.g. Shih et al. 2009), which is comparable to the instantaneous number of positrons with Lorenz factor, $\gamma = 20$ required to explain observed sub-millimeter fluxes. The total thick-target positron yield is about $10^{-2} - 10^{-4}$ per proton of energy above 10 MeV (Kozlovsky et al. 2004), so the total number of positrons produced in a flare should be $\lesssim 10^{31}$. Since the positron lifetime in a dense positron-production site is likely to be less than duration of a flare, the instantaneous positron number of $\sim 10^{31}$ is difficult to achieve, unless we allow a significant fraction of relativistic positrons to escape to and then be trapped at a tenuous coronal part of the flaring loop, where the positron lifetime is much longer.

Synchrotron radiation from relativistic positrons is easily consistent with small sizes if the emission re-

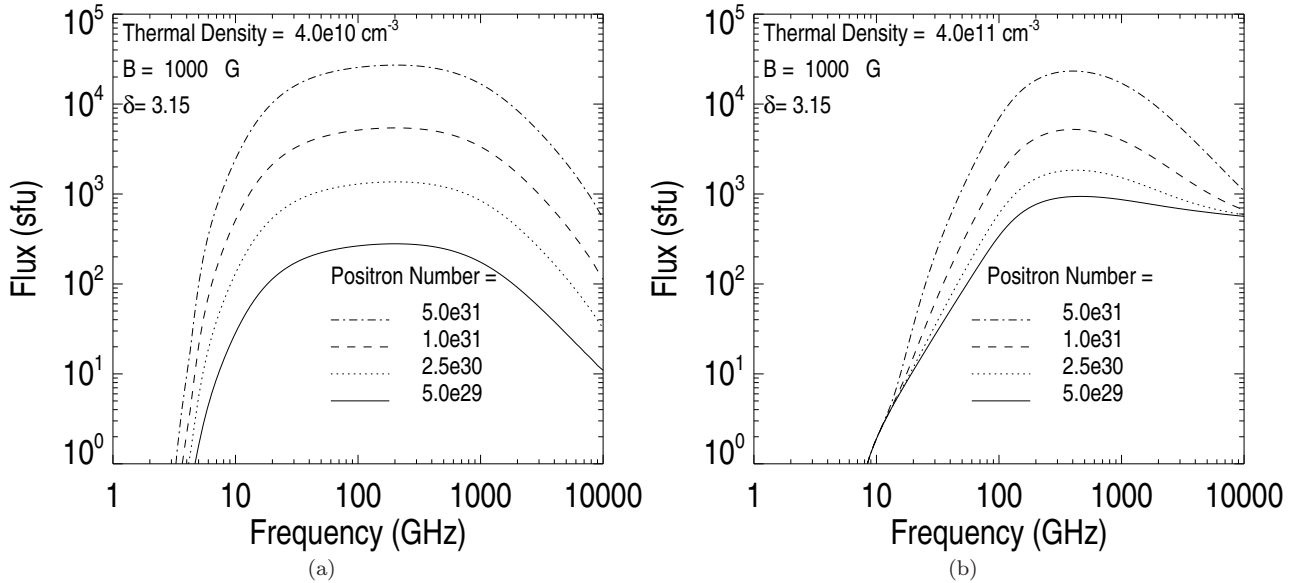


FIG. 3.— Radio spectra produced by synchrotron radiation from relativistic positron plus free-free contribution from a uniform cubic source with a linear size of $20''$ for the total instantaneous positron number $N_{e^+} = 5 \times 10^{29} \dots 5 \times 10^{31}$, with energy $\gamma = 20$ (~ 10 MeV), magnetic field $B = 1000$ G, and the thermal electron density $n_e = 4 \cdot 10^{10} \text{ cm}^{-3}$ (a) and $n_e = 4 \cdot 10^{11} \text{ cm}^{-3}$ (b), and $T_e = 1$ MK.

gion is placed in footpoints of a flaring loop ($\lesssim 7''$) or in a moderate-size ($\lesssim 20''$) coronal flaring loop; such sizes are consistent respectively with hard X-ray measurements of footpoint sizes (Kontar et al. 2008) and radio measurements of the coronal loop sizes (Bastian et al. 1998).

5. DIFFUSIVE RADIATION IN LANGMUIR WAVES WITH LARGE WAVELENGTHS

Unlike the emission processes discussed above, which require dense plasma to produce a sufficiently fast-growing spectrum with frequency, there is a class of wave up-scattering processes, for which a high plasma density is not essential. Inverse Compton scattering of gyro-synchrotron emitted photons is easy to estimate to be inefficient in solar flare conditions because the energy density of electromagnetic emission is much lower than that of the magnetic field, and $\tau_{IC} \ll 1$. Nevertheless, similar processes, in which the role of low-frequency photons is played by plasma waves can be relevant.

Indeed, a flare-accelerated or decay-produced relativistic charged particle moving through the plasma with the turbulent waves experiences random Lorentz forces and so diffuses in space. Accordingly, the corresponding radiative processes are called *diffusive* radiations (e.g., Fleishman 2006). Generally, the diffusive radiations do not produce a spectrum rising with frequency (e.g., Fleishman 2006). An exclusion is DRL for long-wavelength Langmuir waves (Fleishman & Toptygin 2007a,b). In this case the spectrum peaks at frequency $2f_{pe}\gamma^2$, where f_{pe} is the plasma frequency, Figure 4. The spectral index can be as large as 2. The time variability is expected due to nonlinear dynamics of the Langmuir waves, which are known to oscillate under nonlinear wave-wave interactions (e.g. Kontar & Pécseli 2002).

Although this emission process is attractive, it is

unclear whether there are sufficient levels of Langmuir turbulence energy density and relativistic electron/positron numbers to produce the required flux densities. Langmuir waves are effectively generated at shorter wavelengths $\lambda = 2\pi v/\omega_{pe} < 2\pi c/\omega_{pe}$, at the typical resonance phase velocities with the electron beam $v = (0.2 - 0.6)c$ (e.g., Kaplan & Tsytovich 1973; Kontar 2001). Therefore, non-resonant generation of the plasma waves (Dieckmann 2005) or nonlinear wave-wave processes (Kaplan & Tsytovich 1973) transferring energy from small to large wavelength are also implied for this model.

Typically, a large level of Langmuir turbulence would result in strong plasma radio emission due to either coalescence of the plasma waves or scattering/decay into transverse electromagnetic waves. In the DRL model considered here, however, most of the Langmuir turbulence energy resides in long wavelength Langmuir waves, whose wave vectors are small, $k \ll \omega_{pe}/c$. These long wavelength waves cannot coalesce into transverse waves because the conservation of momentum cannot be fulfilled in this three-wave process. Only a minor part of the energy from Langmuir turbulence with $k \gtrsim \omega_{pe}/c$ will be involved in the plasma radiation production, resulting in a modest level of coherent decimeter emission if any, which does not contradict the context radio observations.

To round up the discussion involving the plasma waves, we note that all nonlinear plasma processes including Langmuir waves and *non-relativistic* particles are of little interest here since the fundamental and harmonic plasma frequencies are well below 30 GHz in both chromosphere and corona (Aschwanden et al. 2002).

6. VAVILOV-CHERENKOV RADIATION FROM CHROMOSPHERIC LAYERS

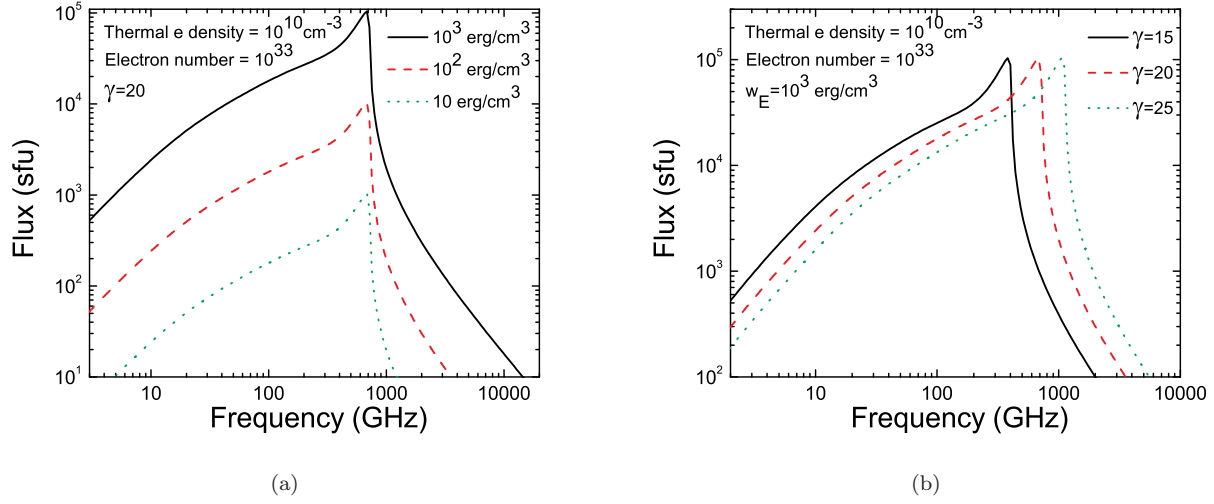


FIG. 4.— DRL spectrum produced by relativistic electrons/positrons in long-wave Langmuir turbulence $\lambda \gg 2\pi c/\omega_{pe}$. (a) Dependency on Langmuir wave energy density, (b) The spectra for different Lorentz factors.

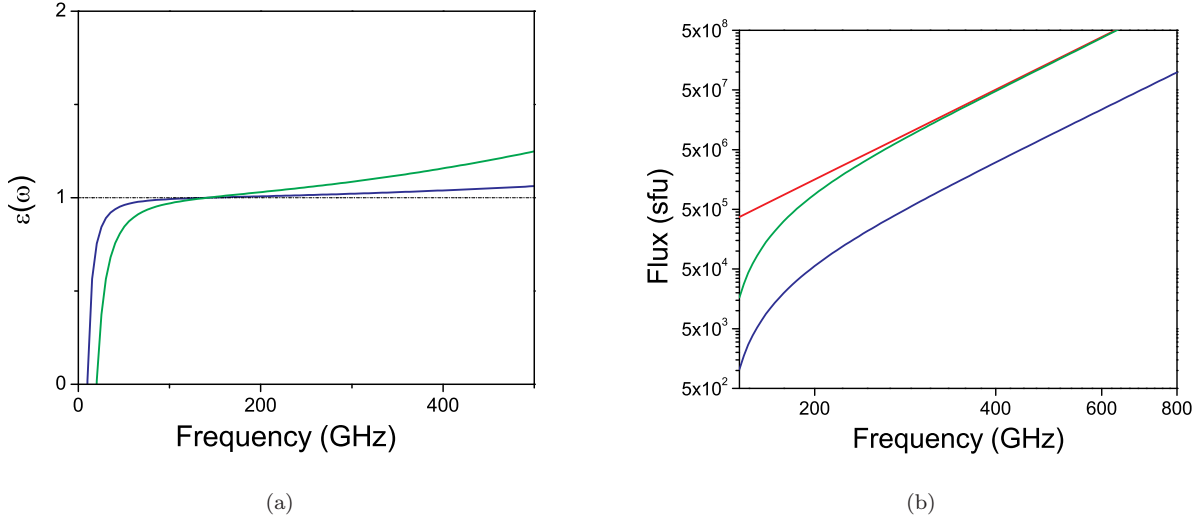


FIG. 5.— (a) A model of plasma dielectric permittivity with molecular line contribution included; (b) Vavilov-Cherenkov radiation produced by fast electrons with a power-law distribution over the velocity—blue and green curves; the red curve is for $\varepsilon(\omega) = 1 + \omega^2/\omega_0^2$, i.e., without standard plasma contribution.

Vavilov-Cherenkov radiation is produced by any charged particle moving faster than the corresponding speed of light in a medium. In fully ionized plasma the high-frequency dielectric permittivity is less than unity, $\varepsilon(\omega) \lesssim 1$. Therefore, the phase velocity of electromagnetic waves $c/\sqrt{\varepsilon(\omega)}$ is larger than the speed of light, c , and the Cherenkov emission does not occur. However, the chromospheric gas is only partly ionized; and there are numerous atoms and molecules whose quantum transitions can make positive contribution to the dielectric permittivity, making Cherenkov radiation possible at certain frequency windows. Charged particle of velocity v emits Cherenkov emission in the medium, where its dielec-

tric permittivity $\varepsilon(\omega)$ is such that $v > c/\sqrt{\varepsilon(\omega)}$. The dielectric permittivity of gases is only slightly more than unity in the optical range [e.g., Hydrogen gas has $(\varepsilon - 1) \sim 2 \cdot 10^{-4}$], so only highly relativistic particles with $v > (1 - 10^{-4})c$ can emit. The situation is however very different in other frequency ranges, near transition frequencies of atoms or molecules: $\varepsilon(\omega)$ goes up and down being considerably larger than one at certain frequency windows, which allows even sub-relativistic electrons to emit Vavilov-Cherenkov radiation.

Each atomic or molecular quantum transition makes a contribution to the dielectric permittivity of

the form of $\delta\varepsilon_{nm}(\omega) = \frac{4\pi n_e e^2}{m_e} \frac{S_{nm}}{(\omega_{nm}^2 - \omega^2) + i\Gamma_{nm}\omega}$, where S_{nm} is the oscillator strength of the transition, ω_{nm} is the transition frequency, Γ_{nm} is the transition decay constant. The resulting dielectric permittivity accounting for plasma (free electrons) and molecular contributions is $\varepsilon(\omega) = 1 - \omega_{pe}^2/\omega^2 + \sum \delta\varepsilon_{nm}$. The exact spectroscopic permittivity depends on the chemical composition of the chromosphere with the sum over all excitation states of corresponding molecules, which is beyond our intention. Here we perform order of magnitude estimates. We assume that there are many atomic/molecular transitions capable of making a contribution to the dielectric properties of gas. Then, we note that the Cherenkov radiation spectrum rises with frequency only if the dielectric permittivity raises with frequency. For example, the energy level distribution between the rotational levels of chromospheric molecules can be assumed to have a Boltzmann distribution with the gas temperature T , therefore population densities will have maxima at energy levels above the THz range increasing to about $k_B T$. Thus, we adopt the mean molecular contribution to the dielectric permittivity to have the *model* form ω^2/ω_0^2 , where ω_0 is an unknown constant.

Assuming a power-law spectrum of fast electrons $n_e(v) = AN_0 v_0^{\beta-1}/v^\beta$, $v < c$, where N_0 is the total number of electrons with velocity above minimum velocity v_0 , β is the spectral index, and A is a dimensionless normalization constant of order of unity, the Cherenkov emission yields flux at Earth:

$$F_f = \frac{10^{19}}{4\pi R_{\text{au}}^2} \frac{(2\pi)^2 AN_0 e^2 f v_0^{\beta-1}}{c^\beta} \times \left[\frac{2\varepsilon^{(\beta-2)/2}}{\beta(\beta-2)} + \frac{1}{\beta\varepsilon} - \frac{1}{\beta-2} \right] \quad (\text{sfu}). \quad (1)$$

Figure 5(a) displays the model dielectric permittivity rising with frequency as described, while Figure 5(b) shows the corresponding Cherenkov spectra. The spectrum shape and the flux density level allow this emission to be easily reconciled mechanism with observations for typical numbers of accelerated electrons. The model flux density is much larger than observed, being 5×10^7 sfu at 400 GHz, which allows us to relax the number of radiating electrons or/and add some free-free absorption to the model. Given that the emission is from compact footpoints $< 10''$, where energetic particles interact with the chromosphere, we conclude that the Cherenkov emission is fully consistent with the observations of the rising sub-THz component of large solar flares. The time variability requires corresponding fluctuations of the electron distribution function, similar to sub-second variations of microwave GS or HXR radiations.

7. DISCUSSION AND CONCLUSIONS

We have analyzed a number of emission processes, which are capable of producing radiation at the sub-millimeter wavelengths: free-free emission, gyrosynchrotron and synchrotron processes, diffusive radiation, and Vavilov-Cherenkov process. Having in mind

the characteristic ranges of parameters of a solar flare region, we calculated the spectra for each process discussed in the paper. Although current observations at two frequencies only do not provide us with detailed spectral shape, we estimate the range of flux levels and spectral indices for each model and compare them with the observations.

It is likely that the sub-THz emission originates from more than a single source and more than one mechanism is involved. Free-free emission is a plausible candidate in many cases, at least for large sources observed by Lüthi et al. (2004a,b). The free-free emission is clearly always present, so other mechanisms build additional contributions on top of the free-free component. Gyrosynchrotron/synchrotron emission is likely to play a role in moderate events and also as the extension of normal microwave bursts, which falls with frequency. The role of DRL is less clear since the level of long-wavelength Langmuir waves is yet unknown in flares. Finally, the Vavilov-Cherenkov emission from compact sources located at the chromospheric level seems to be a plausible process to account for the rising with frequency sub-mm component of large flares. Indeed, the dielectric permittivity of partially ionized plasma is known to fluctuate around unity due to atomic and molecular transition contributions. When the flare-accelerated electrons are present, they will produce Cherenkov radiation at all frequency windows (including IR, viz, and UV bands) where the dielectric permittivity is (even marginally) above unity, giving rise to a radiation spectrum raising with frequency for (mean) dielectric permittivity increasing with frequency.

The available constraints on sub-THz source sizes, time variability, and spectral index are not yet fully reliable particularly because the ground-based sub-THz observations are extremely difficult to calibrate due to strongly variable atmospheric opacity. Further progress in understanding the physics of sub-THz emission from flares requires observations a) with a more complete spectral coverage at the sub-mm range (preferably well-calibrated space-based observations) and b) polarization measurements. Nevertheless, the sub-THz spectral window can be extremely informative, e.g., for diagnostics of the chromospheric chemical composition if the role of the Vavilov-Cherenkov emission is confirmed. This calls for a new project mounting a sub-THz receivers/interferometers, combining good sensitivity with high spatial resolution, on a space mission, complementing on-going efforts in the microwave range.

This work (GDF) was supported in part by NSF grants ATM-0707319 and AST-0908344, and NASA grant 09-HGI09-0057, and by the Russian Foundation for Basic Research, grants 08-02-92228, 09-02-00226, and 09-02-00624. EPK gratefully acknowledges comments by Lyndsay Fletcher and financial support by a STFC (UK) rolling grant, STFC Advanced Fellowship, the Leverhulme Trust and by the European Commission through the SOLAIRE Network (MTRN-CT-2006-035484).

REFERENCES

- Aschwanden, M. J. 2005, *Physics of the Solar Corona. An Introduction with Problems and Solutions* (2nd edition)
- Aschwanden, M. J., Brown, J. C., & Kontar, E. P. 2002, *Sol. Phys.*, 210, 383
- Aschwanden, M. J., Kliem, B., Schwarz, U., Kurths, J., Dennis, B. R., & Schwartz, R. A. 1998, *ApJ*, 505, 941
- Bastian, T. S., Benz, A. O., & Gary, D. E. 1998, *ARA&A*, 36, 131
- Bazylev, V. A. & Zhevago, N. K. 1987, Moscow Izdatel Nauka
- Brown, J. C. & Kontar, E. P. 2005, *Advances in Space Research*, 35, 1675
- Brown, J. C., Kontar, E. P., & Veronig, A. M. 2007, in *Lecture Notes in Physics*, Berlin Springer Verlag, Vol. 725, *Lecture Notes in Physics*, Berlin Springer Verlag, ed. K.-L. Klein & A. L. MacKinnon, 65–+
- Cristiani, G., Giménez de Castro, C. G., Mandrini, C. H., Machado, M. E., Silva, I. D. B. E., Kaufmann, P., & Rovira, M. G. 2008, *A&A*, 492, 215
- Dennis, B. R. & Schwartz, R. A. 1989, *Sol. Phys.*, 121, 75
- Dieckmann, M. E. 2005, *Physical Review Letters*, 94, 155001
- Edwin, P. M. & Roberts, B. 1983, *Sol. Phys.*, 88, 179
- Emslie, A. G., Kontar, E. P., Krucker, S., & Lin, R. P. 2003, *ApJ*, 595, L107
- Fleishman, G. D. 2006, *ApJ*, 638, 348
- Fleishman, G. D., Bastian, T. S., & Gary, D. E. 2008, *ApJ*, 684, 1433
- Fleishman, G. D. & Toptygin, I. N. 2007a, *MNRAS*, 381, 1473
- , 2007b, *Phys. Rev. E*, 76, 017401
- Kaplan, S. A. & Tsytovich, V. N. 1973, *Plasma astrophysics* (International Series of Monographs in Natural Philosophy, Oxford: Pergamon Press, 1973)
- Kaufmann, P., Giménez de Castro, C. G., Correia, E., Costa, J. E. R., Raulin, J.-P., & Válio, A. S. 2009a, *ApJ*, 697, 420
- Kaufmann, P., Raulin, J.-P., Correia, E., Costa, J. E. R., de Castro, C. G. G., Silva, A. V. R., Levato, H., Rovira, M., Mandrini, C., Fernández-Borda, R., & Bauer, O. H. 2001, *ApJ*, 548, L95
- Kaufmann, P., Raulin, J.-P., de Castro, C. G. G., Levato, H., Gary, D. E., Costa, J. E. R., Marun, A., Pereyra, P., Silva, A. V. R., & Correia, E. 2004, *ApJ*, 603, L121
- Kaufmann, P., Trottet, G., Giménez de Castro, C. G., Raulin, J.-P., Krucker, S., Shih, A. Y., & Levato, H. 2009b, *Sol. Phys.*, 255, 131
- Kašparová, J., Karlický, M., Kontar, E. P., Schwartz, R. A., & Dennis, B. R. 2005, *Sol. Phys.*, 232, 63
- Kiplinger, A. L., Dennis, B. R., Frost, K. J., & Orwig, L. E. 1984, *ApJ*, 287, L105
- Kontar, E. P. 2001, *Sol. Phys.*, 202, 131
- Kontar, E. P., Hannah, I. G., & MacKinnon, A. L. 2008, *A&A*, 489, L57
- Kontar, E. P. & Pécseli, H. L. 2002, *Phys. Rev. E*, 65, 066408
- Kozlovsky, B., Murphy, R. J., & Ramaty, R. 2002, *ApJS*, 141, 523
- Kozlovsky, B., Murphy, R. J., & Share, G. H. 2004, *ApJ*, 604, 892
- Kramer, C., Degiacomi, C. G., Graf, U. U., Hills, R. E., Miller, M., Schieder, R., Schneider, N., Stutzki, J., & Winnewisser, G. F. 1998, in *Society of Photo-Optical Instrumentation Engineers (SPIE) Conference Series*, Vol. 3357, *Society of Photo-Optical Instrumentation Engineers (SPIE) Conference Series*, ed. T. G. Phillips, 711–720
- Lingenfelter, R. E. & Ramaty, R. 1967, *Planet. Space Sci.*, 15, 1303
- Lüthi, T., Lüdi, A., & Magun, A. 2004a, *A&A*, 420, 361
- Lüthi, T., Magun, A., & Miller, M. 2004b, *A&A*, 415, 1123
- Nakariakov, V. M. & Verwichte, E. 2005, *Living Reviews in Solar Physics*, 2, 3
- Nindos, A., Aurass, H., Klein, K.-L., & Trottet, G. 2008, *Sol. Phys.*, 253, 3
- Shih, A. Y., Lin, R. P., & Smith, D. M. 2009, *ApJ*, 698, L152
- Silva, A. V. R., Share, G. H., Murphy, R. J., Costa, J. E. R., de Castro, C. G. G., Raulin, J.-P., & Kaufmann, P. 2007, *Sol. Phys.*, 245, 311
- Trottet, G., Krucker, S., Lüthi, T., & Magun, A. 2008, *ApJ*, 678, 509
- Trottet, G., Raulin, J.-P., Kaufmann, P., Siarkowski, M., Klein, K.-L., & Gary, D. E. 2002, *A&A*, 381, 694